Supplement of Hydrol. Earth Syst. Sci., 27, 3485–3504, 2023
https://doi.org/10.5194/hess-27-3485-2023-supplement

Hydrology and Earth System Sciences
Open Access
EGU

Supplement of

Calibrating macroscale hydrological models in poorly gauged and heavily regulated basins

Dung Trung Vu et al.

Correspondence to: Dung Trung Vu (trungdung_vu@mymail.sutd.edu.sg)

Table S1. Design specifications of the hydropower dams on the mainstream of the Lancang River. Data retrieved from Do et al. (2020).

Name	COM	Height (m)	MWL (m)	DWL (m)	MWA (km^2)	Dead storage (MCM)	Full storage (MCM)	Hydropower capacity (MW)
Jinghong	2009	108	602	595	510	810	1119	1750
Nuozhadu	2014	262	812	756	320	10414	21749	5850
Dachaoshan	2003	115	899	887	826	465	740	1350
Manwan	1992	132	994	982	415	630	887	1670
Xiaowan	2010	292	1236	1162	194	4750	14645	4200
Gongguoqiao	2012	105	1319	1311	343	196	316	900
Miaowei	2016	140	1408	1373	171	359	660	1400
Dahuaqiao	2018	106	1477	1466	148	252	293	920
Huangdeng	2017	203	1619	1604	199	1031	1418	1900
Wunonglong	2018	138	1906	1894	163	236	272	990

COM Year of commission
MWL Maximum water level
DWL Dead water level
MWA Maximum water surface area

Table S2. List of Landsat-5 images used to identify the river cross-section at the virtual station.

ID	Collection Date (dd/mm/yyyy)	River Width (m)	Water Level* (m)
LT05_L1TP_129046_20080929_20161029_01_T1	29/09/2008	240	298.36
LT05_L1TP_129046_20081015_20161029_01_T1	15/10/2008	240	297.47
LT05_L1TP_129046_20081202_20170111_01_T1	02/12/2008	210	291.89
LT05_L1TP_129046_20081218_20170111_01_T1	18/12/20008	210	290.75
LT05_L1TP_129046_20090119_20161028_01_T1	19/01/2009	210	288.80
LT05_L1TP_129046_20090220_20161027_01_T1	20/02/2009	180	287.39
LT05_L1TP_129046_20090308_20161029_01_T1	08/03/2009	180	286.77
LT05_L1TP_129046_20091018_20161019_01_T1	18/10/2009	210	293.50
LT05_L1TP_129046_20091103_20161023_01_T1	03/11/2009	210	292.51
LT05_L1TP_129046_20091205_20161017_01_T1	05/12/2009	210	288.93
LT05_L1TP_129046_20100207_20161017_01_T1	07/02/2010	180	285.88
LT05_L1TP_129046_20100223_20161016_01_T1	23/02/2010	180	284.06
LT05_L1TP_129046_20100428_20161015_01_T1	28/04/2010	180	287.85
LT05_L1TP_129046_20100514_20161015_01_T1	14/05/2010	180	287.22
LT05_L1TP_129046_20100903_20161014_01_T1	03/09/2010	240	297.37
LT05_L1TP_129046_20101106_20161012_01_T1	06/11/2010	210	293.59
LT05_L1TP_129046_20110125_20161010_01_T1	25/01/2011	210	288.38
LT05_L1TP_129046_20110210_20161010_01_T1	10/02/2011	180	287.45
LT05_L1TP_129046_20110415_20161209_01_T1	15/04/2011	180	287.74

* obtained by Jason-2/3 on the corresponding day

Table S3. Model calibration performance calculated for twelve selected solutions, i.e., those yielding the top 25% performance in terms of NSE, TRMSE, MSDE, and ROCE. The performance metrics are calculated by comparing simulated and remote-sensed discharge at the virtual station.

No.	NSE	TRMSE	MSDE	ROCE
1	0.689	3.353	891526	0.035
2	0.689	3.353	891388	0.035
3	0.689	3.354	890904	0.035
4	0.688	3.360	897298	0.040
5	0.687	3.356	891553	0.030
6	0.687	3.345	908805	0.033
7	0.687	3.345	908805	0.033
8	0.686	3.343	891400	0.036
9	0.686	3.343	891400	0.036
10	0.686	3.343	890948	0.036
11	0.686	3.343	891457	0.036
12	0.686	3.337	891369	0.039

Table S4. Model validation performance calculated for the twelve selected solutions. The performance metrics are calculated by comparing simulated and observed discharge at Chiang Saen station.

No.	NSE	TRMSE	MSDE	ROCE
1	0.616	3.908	1062099	0.169
2	0.608	3.919	1058180	0.183
3	0.608	3.919	1058419	0.183
4	0.608	3.920	1057966	0.183
5	0.599	3.891	1058223	0.170
6	0.598	3.904	1058282	0.177
7	0.598	3.904	1058282	0.177
8	0.598	3.906	1058083	0.178
9	0.598	3.905	1058305	0.178
10	0.596	3.935	1058645	0.195
11	0.594	3.911	1071282	0.187
12	0.594	3.911	1071282	0.187

Table S5. Model calibration performance, calculated for the 58 selected solutions (the Pareto front) from model calibration. The performance metrics are calculated between simulated and remote-sensed discharge at the virtual station.

No.	NSE	TRMSE	MSDE	ROCE	No.	NSE	TRMSE	MSDE	ROCE
1	0.698	3.375	1065802	0.041	30	0.688	3.330	1119978	0.027
2	0.697	3.363	1064265	0.046	31	0.688	3.372	883766	0.038
3	0.696	3.420	1104404	0.013	32	0.687	3.265	1240258	0.057
4	0.696	3.333	1296485	0.022	33	0.687	3.356	891553	0.030
5	0.696	3.374	1061290	0.042	34	0.687	3.336	897516	0.047
6	0.695	3.377	1060950	0.041	35	0.687	3.410	884122	0.035
7	0.695	3.379	1039961	0.040	36	0.687	3.407	885826	0.036
8	0.695	3.301	1298463	0.032	37	0.687	3.345	908805	0.033
9	0.694	3.366	1172060	0.028	38	0.687	3.398	883010	0.037
10	0.694	3.300	1296746	0.032	39	0.686	3.432	854452	0.038
11	0.694	3.301	1297546	0.032	40	0.686	3.343	891400	0.036
12	0.693	3.329	973419	0.041	41	0.686	3.343	890948	0.036
13	0.693	3.324	963126	0.041	42	0.686	3.420	883425	0.037
14	0.693	3.311	1300094	0.024	43	0.686	3.337	891369	0.039
15	0.692	3.310	1298422	0.024	44	0.685	3.271	1238422	0.059
16	0.692	3.303	1121617	0.032	45	0.685	3.447	864589	0.037
17	0.692	3.305	1118386	0.031	46	0.685	3.465	858494	0.037
18	0.692	3.286	1237423	0.039	47	0.681	3.422	880224	0.045
19	0.691	3.307	977172	0.043	48	0.680	3.348	1286568	0.024
20	0.691	3.387	1170933	0.018	49	0.679	3.363	1269557	0.018
21	0.691	3.308	1230897	0.025	50	0.679	3.379	1254975	0.014
22	0.690	3.386	1174178	0.019	51	0.673	3.452	793084	0.037
23	0.690	3.387	1174042	0.019	52	0.672	3.425	792973	0.028
24	0.690	3.295	1244238	0.038	53	0.670	3.428	793443	0.026
25	0.690	3.324	962490	0.049	54	0.670	3.428	793443	0.026
26	0.689	3.299	1244769	0.037	55	0.670	3.428	793443	0.026
27	0.689	3.353	891526	0.035	56	0.670	3.428	793443	0.026
28	0.689	3.353	891388	0.035	57	0.656	3.545	1285269	0.007
29	0.689	3.354	890904	0.035	58	0.646	3.588	892415	0.001

Table S6. Model validation performance, calculated for the 58 selected solutions (the Pareto front) from model calibration. The performance metrics are calculated between simulated and observed discharge at Chiang Saen station.

No.	NSE	TRMSE	MSDE	ROCE	No.	NSE	TRMSE	MSDE	ROCE
1	0.637	3.928	989984	0.174	30	0.594	3.911	1071282	0.187
2	0.635	3.897	988499	0.170	31	0.592	3.871	1211314	0.223
3	0.634	3.924	1002652	0.173	32	0.592	3.872	1211245	0.223
4	0.632	3.716	1093794	0.139	33	0.591	3.846	1335416	0.117
5	0.631	3.745	1093664	0.157	34	0.588	4.032	993374	0.201
6	0.625	3.944	1047262	0.158	35	0.586	3.845	1336296	0.123
7	0.624	3.731	1094157	0.152	36	0.581	4.041	994241	0.206
8	0.623	3.733	1094213	0.154	37	0.581	4.041	994241	0.206
9	0.622	3.737	1081727	0.156	38	0.581	4.041	994241	0.206
10	0.621	3.967	1050516	0.180	39	0.581	4.041	994241	0.206
11	0.620	3.851	1108955	0.143	40	0.574	3.923	1334334	0.174
12	0.619	3.957	1052596	0.180	41	0.570	3.950	1376977	0.192
13	0.619	3.948	1050599	0.177	42	0.569	3.928	1337789	0.177
14	0.619	3.963	1051327	0.183	43	0.568	3.960	949657	0.292
15	0.618	3.861	1059505	0.148	44	0.567	3.932	1337865	0.179
16	0.616	3.927	1051718	0.176	45	0.567	3.947	1248912	0.193
17	0.614	3.885	1119650	0.166	46	0.567	3.942	1386466	0.187
18	0.613	3.880	1112699	0.165	47	0.566	3.944	1386968	0.187
19	0.610	3.842	1207660	0.197	48	0.566	3.953	1246566	0.196
20	0.609	4.022	990455	0.180	49	0.566	3.942	1388012	0.188
21	0.608	3.919	1058180	0.183	50	0.564	4.001	1389071	0.218
22	0.608	3.919	1058419	0.183	51	0.561	3.970	1327052	0.214
23	0.605	3.883	1088908	0.171	52	0.557	3.977	1246317	0.205
24	0.602	3.847	1119397	0.159	53	0.553	3.981	1318489	0.243
25	0.599	3.891	1058223	0.170	54	0.552	3.975	1388532	0.211
26	0.598	3.904	1058282	0.177	55	0.551	3.973	1389883	0.210
27	0.598	3.841	1133345	0.236	56	0.545	3.992	1368735	0.216
28	0.598	3.906	1058083	0.178	57	0.539	4.015	1353742	0.232
29	0.596	3.935	1058645	0.195	58	0.512	4.190	1053505	0.276

Figure S1. Approach for constructing the river cross-section at the virtual station (a) and elements of the river cross-section used to construct the rating curve (b). Note that the approach builds on multiple satellite data, namely DEM, altimetry, and river width (derived from Landsat images).

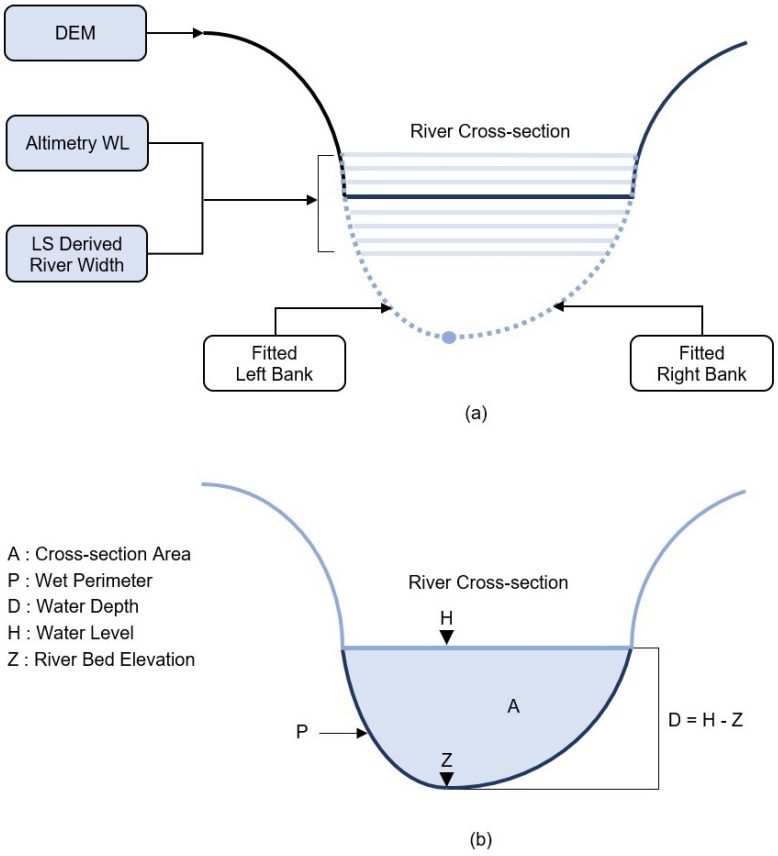

Figure S2. Panels (a-d) show the results of four alternative cross-sections, created by moving the one at the location of the virtual station (reported in Figure 4a and marked by VS in the panel (e) and (f)) 30 and 60m (1 and 2 cells) both upstream and downstream. The five cross-sections are plotted together in panel (e), and a 3D visualization is provided in panel (f).

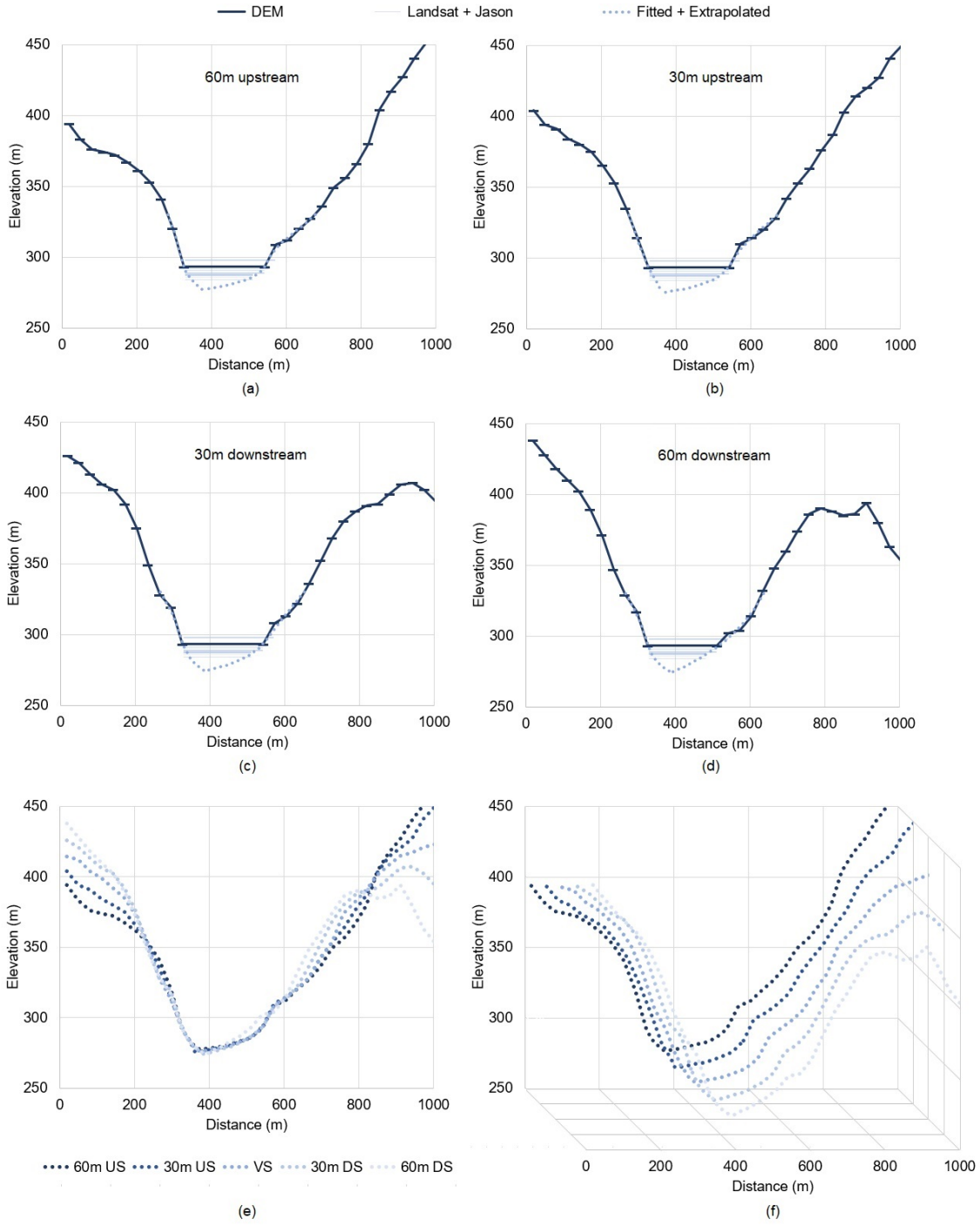

Figure S3. Comparison between remote sensed (RS) and simulated discharge at the virtual station. The range of variability of the RS discharge is represented by the medium blue band, while the range of simulated discharge (corresponding to a range of Manning's coefficient $n \in$ [0.04-0.052]) is represented by the light green band. The RS discharge estimated with $n = 0.046$ is illustrated by the dark blue line. Finally, the dotted orange line illustrates the discharge estimated by scaling the discharge observed at Chiang Saen by the area ratio.

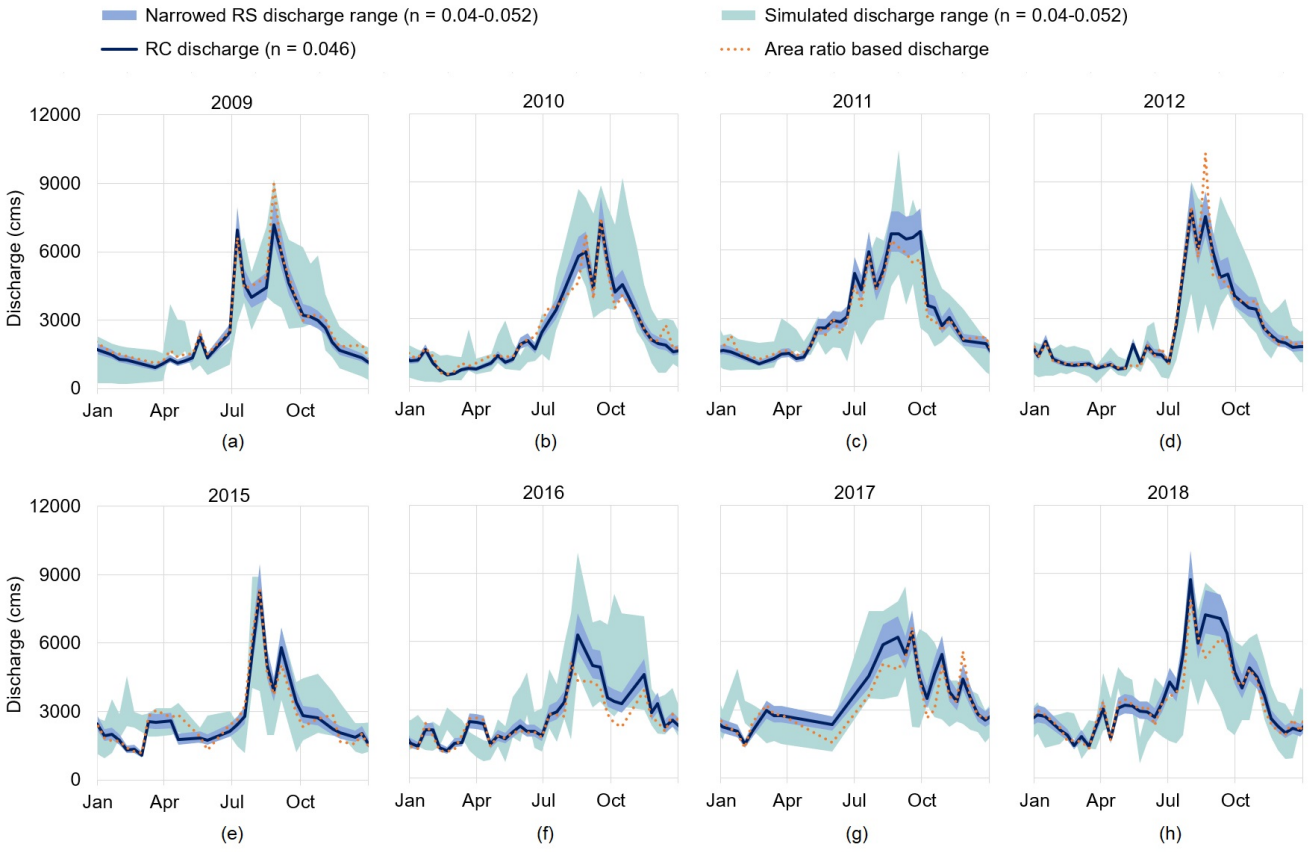

Figure S4. Comparison of discharge time series obtained during calibration at the virtual station (a) and validation at Chiang Saen station (b). The dark green band depicts the range of variability of 58 selected solutions (corresponding to the Pareto front), while the light green band corresponds to the range of variability of 40 solutions selected in the sensitivity analysis. In panel (a), the dark blue line represents the remote sensed discharge at the virtual station (with $n = 0.046$), while the dotted orange line corresponds to the discharge estimated by scaling the discharge observed at Chiang Saen by the area ratio. In panel (b), the dotted orange line illustrates the observed discharge at Chiang Saen.

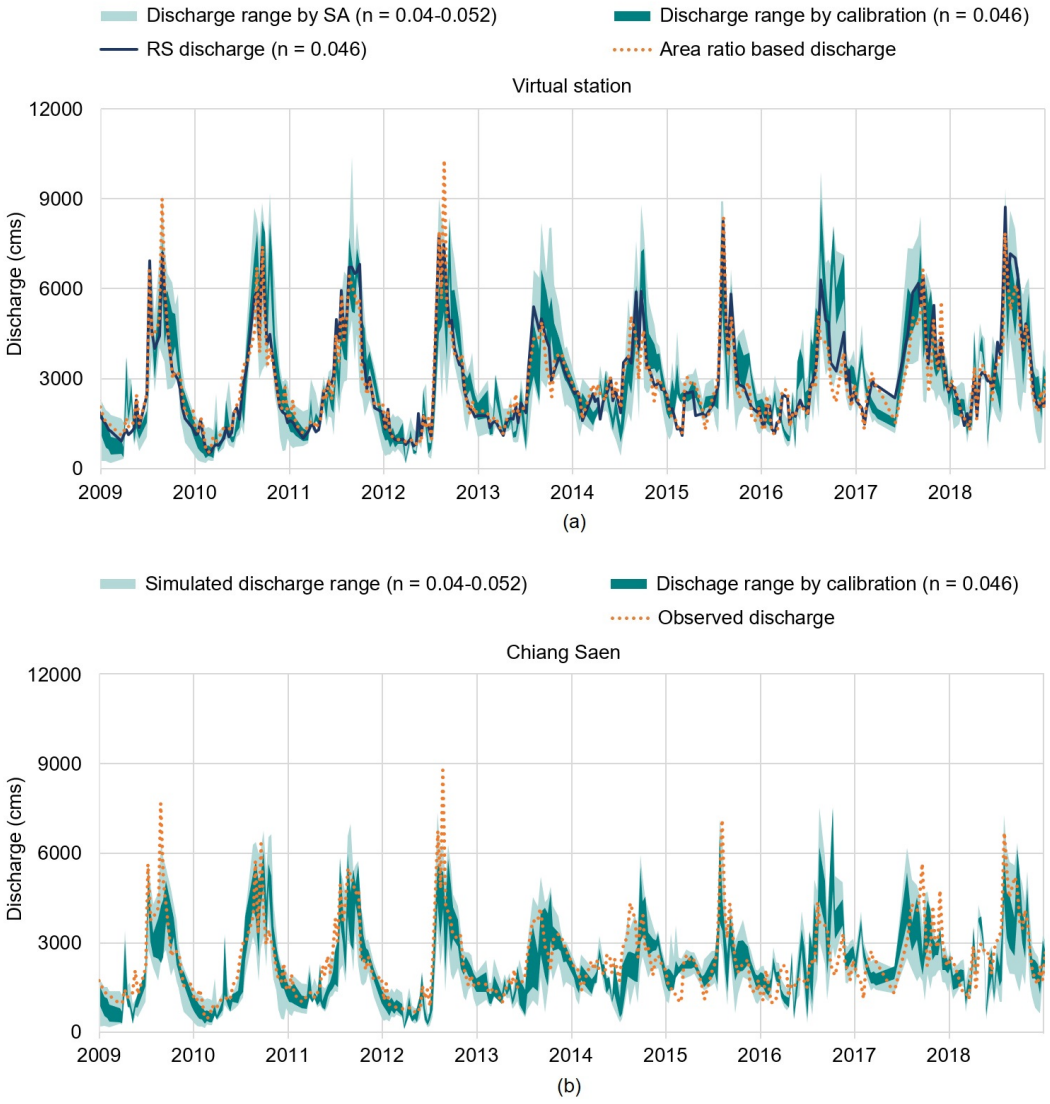

Figure S5. VIC-Res parameters after model calibration. In panel (a), solutions were selected by intersecting the four top 25% parameterizations for each performance metric. In panel (b), the highlighted parameterizations correspond to the Pareto solutions.

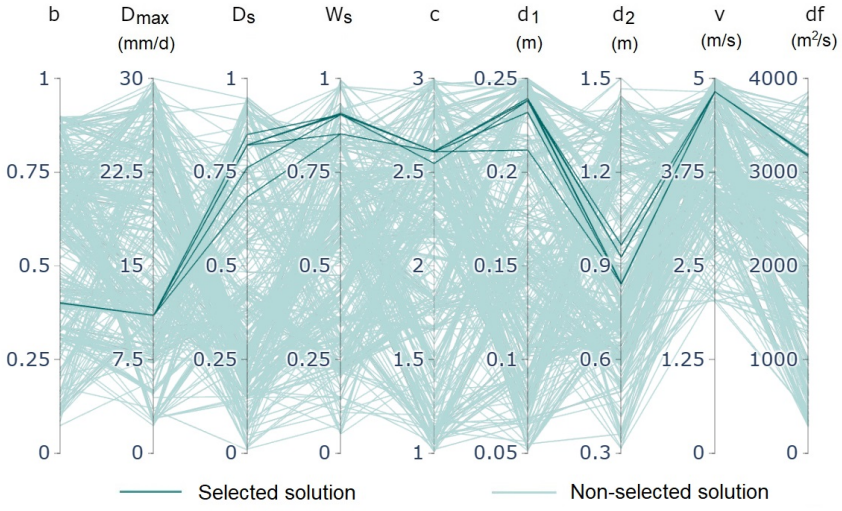

(a)

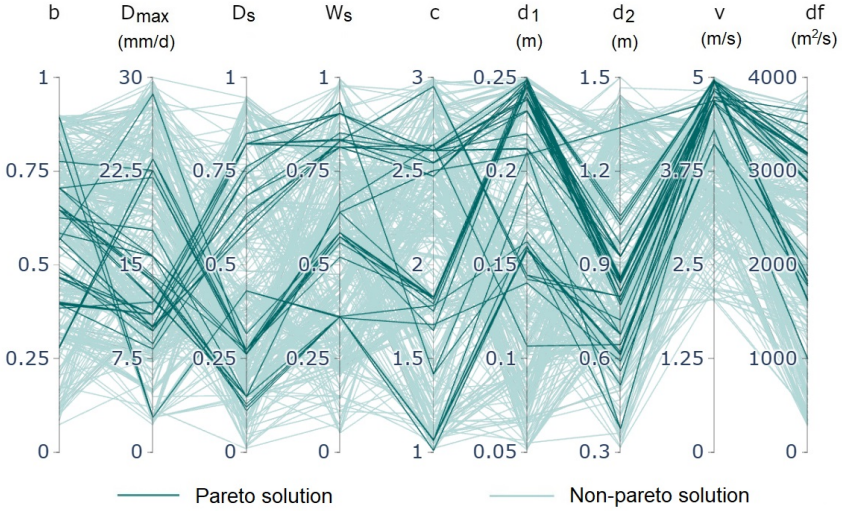

(b)

5 References

Do, P., Tian, F., Zhu, T., Zohidov, B., Ni, G., Lu, H., and Liu, H.: Exploring synergies in the water-food-energy nexus by using an integrated hydro-economic optimization model for the Lancang-Mekong River Basin, Science of The Total Environment, 728, 137 996, https://doi.org/10.1016/j.scitotenv.2020.137996, 2020.